The electrostatic potential within which the electron moves will differ from the usual Coulomb form it would assume if the proton were strictly a point charge. The actual potential energy may be calculated for a known proton charge-density distribution from the relation

$$V(r) = -(4\pi e/r) \int_0^r \rho(r')r'^2\,dr' - (4\pi e) \int_r^\infty \rho(r')r'dr' \qquad (2)$$

where $V(r)$ is the potential energy and the other symbols have the same meaning as before. If the integrals in Eq. 2 are evaluated with the proton density distribution of Eq. 1, the result is

$$V(r) = -e^2/r + (e^2/r)\,[1 + (\alpha r/2)] \exp(-\alpha r) \qquad (3)$$

Therefore, the electrostatic potential energy consists of the usual attractive Coulomb term plus the short-ranged term $V'(r)$ where

$$V'(r) = (e^2/r)\,[1 + (\alpha r/2)] \exp(-\alpha r) \qquad (4)$$

As a result of this additional term, the electronic energy levels will be shifted from the values for hydrogen by an amount given, to a first approximation, by $V'_{nlm,\,nlm}$, the expectation value of $V'(r)$ in the state whose quantum numbers are n, l, and m (*2*). Calculation of this expectation value for the $1s$ and $2s$ states gives

$$V'_{100,\,100} = (1.52 \times 10^{-10})\ e^2/a_0$$
$$V'_{200,\,200} = (0.19 \times 10^{-10})\ e^2/a_0$$

where $a_0 = 0.53 \times 10^{-8}$ cm is the Bohr radius. Since the energy of the state of principal quantum number n is given by

$$E_n = -e^2/(2n^2a_0)$$

these shifts represent approximately 3.0 and 1.5 parts in 10^{10} of the corresponding unperturbed energy values. The term $V'(r)$ also causes a splitting of the $2s$ and $2p$ energy levels which is of the same order of magnitude as $V'_{200,\,200}$ and which corresponds to a frequency of approximately 0.10 megacycle. It is of interest to note that this frequency is of the same order of magnitude as the still-unexplained difference between the measured and the field theoretical values of the Lamb shift for these levels (*3*).

Calculations with charge density distributions other than the exponential form of Eq. 1 lead to comparable values of the aforementioned effects.

WILLIAM S. PORTER
Department of Physics, Bucknell University, Lewisburg, Pennsylvania

20 MARCH 1964

References

1. R. Hofstadter, *Ann. Rev. Nucl. Sci.* **7**, 231 (1957).
2. R. H. Dicke and J. P. Wittke, *Introduction to Quantum Mechanics* (Addison-Wesley, Reading, Mass., 1960), pp. 226–258.
3. A. J. Layzer, *Phys. Rev. Letters* **4**, 580 (1960).

4 December 1963

Simultaneous Studies of Firing Patterns in Several Neurons

Abstract. *A tungsten microelectrode with several small holes burnt in the vinyl insulation enables the action potentials from several adjacent neurons to be observed simultaneously. A digital computer is used to separate the contributions of each neuron by examining and classifying the waveforms of the action potentials. These methods allow studies to be made of interactions between neurons that lie close together.*

The extent to which physically contiguous neurons form domains or functional aggregates is a fundamental problem in studying the organization of the central nervous system. That such domains exist in sensory cortical regions has been shown by electrophysiological methods: a "cylinder," measuring 200 μ in diameter and running through the depths of the cortex, forms some sort of functional unit in the processing of sensory information (*1*, *2*). Elaboration of neural interactions within such a functional aggregate has proved difficult. A macroelectrode picks up the summated (slow) activity of thousands to millions of neurons while a microelectrode usually picks up the electrical activity of one cell at a time. It is obviously necessary to bridge these extremes by recording simultaneously and separably the electrical activity of small clusters of neurons.

Some data on the simultaneous activity of two neurons have been obtained from microelectrode recordings which show two spike trains that are distinguishable because of widely different amplitude (*2*, *3*). Other authors have used several microelectrodes independently inserted into the structure being studied (*4*). With this technique it is difficult to ensure that the neurons under study are closely spaced because of deformation of the tissues and flexibility of the microelectrodes. In addition, the neurons are more likely to be damaged as the number of microelectrodes is increased. Changes in neuron connectivity, pressure changes, and alterations in microcirculation are not easily controlled or evaluated by the experimenter. Accordingly, we approached the problem by developing a single microelectrode that would allow three to five different trains of action potentials to be recorded simultaneously. Since the geometry relative to the electrode differs for each neuron under observation, the various action potentials may be distinguished by their waveform.

While working with very large (30 to 50 μ) tungsten microelectrodes we frequently observed the activities of a number of neurons, unfortunately with very low amplitudes because of the large open area of the electrode. Tungsten microelectrodes with a smaller open area (5 to 10 μ) produce excellent action-potential amplitudes, but allow only one or two neurons to be observed simultaneously. Obviously, we required an electrode with a total open area comparable to the usual 5- to 10-μ electrode, but with this open area distributed over some 100 μ of the shaft.

Such a "distributed area" microelectrode can be produced from the usual 10-μ tungsten microelectrode (*5*) by damaging the vinyl insulation. Under 100-power magnification, the tip of the electrode is inserted into a hanging drop of clean mineral oil for protection. Another microelectrode is brought up at right angles to within 5 to 10 μ of the shaft some 50 μ from the tip, and a short series of sparks from a Tesla coil (*6*) is applied between the two electrodes. The intensity and duration of the sparks must be determined experimentally. By this procedure several small holes are burned in the vinyl insulation at random points along the first 100 μ of the microelectrode shaft. When tested, the electrode shows bubbling at these several points as well as at the tip. By proper design of the various electrode holders and saline test bath, the entire test-spark-test procedure for an electrode can be carried out under a microscope in a few minutes.

Typical action potential data observed with the distributed area tungsten microelectrode are shown in Fig. 1*A*. This example is taken from the dorsal cochlear nucleus of a cat anesthetized with Nembutal; similar results have been obtained in various brain-stem, cerebellar, and cortical lo-

cations. The electrode will pick up a particular train of action potentials over some 200 μ of electrode displacement. Thus neurons giving rise to a typical multiple-unit recording probably lie within a sphere 200 μ in diameter. In Fig. 1*B* the same data are presented with a faster time base, so that the waveform of each action potential is visible. The oscilloscope was triggered as each spike crossed an amplitude setting; the initial rise of the spike from baseline is therefore not shown.

The differences in waveform evident in Fig. 1B can be used to separate the data recorded by the distributed area microelectrode into the electrical activities of each of several neurons. Such a sorting of the composite electrical record could be performed by hand measurement on film strips (*7*). A less tedious procedure was accomplished by the use of TX-2, an extremely large and powerful general purpose computer (*8*).

As the data are played back from analog tape, each action potential is sensed by the computer, and 32 digital samples (points) straddling the waveform are placed into the computer memory. Simultaneously, the time of occurrence of each action potential as well as of each stimulus marker is stored. A total of 7000 action potentials can be accommodated.

The program sorts the action potential waveforms by comparing each one to some particular action potential which has been chosen as the "standard." The comparison is accomplished by calculating a weighted mean square difference over the 32 digital samples. The single positive number thus obtained for each comparison is a measure of dissimilarity to the "standard" waveform. If the waveforms are identical this dissimilarity number is zero; differences between the waveforms lead to a positive dissimilarity number. This process is considerably more general than the sorting of action potential amplitudes alone, since it can distinguish two action potentials of similar amplitude but different waveshape. (Such data are shown in Fig. 1, *A* and *B*.)

Although the population of waveforms for a typical multiple-unit recording could be uniformly distributed across a range of dissimilarity numbers, usually there is sufficient clustering to allow the action potential waveforms to be sorted into several groups. Various options in the program allow overlap between such clusters to be minimized. For example, any of the action potentials in the data may be tried as "standard" waveforms. Alternatively, a number of waveforms which are most similar to a "standard" can be averaged together to generate a new "standard" waveform in an iterative sorting procedure. Each of the 32 points comprising a waveform can be individually weighted during computation of the dissimilarity number, thus emphasizing various portions of the waveform.

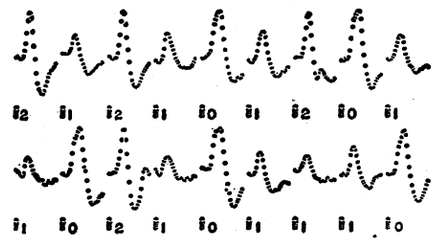

Fig. 2. A print-out which is used to monitor the waveform classifications achieved by the program. (The large numerals were added by hand.)

The most useful sorting procedure identifies one "most similar" group of waveforms in those cases when the population has only a bimodal distribution as a function of the dissimilarity number, and then removes the identified group of waveforms from further calculations. (Only a waveform group defined by a small dissimilarity number is unique; there are many differences between waveforms which can produce a large dissimilarity number.) An example of this type of sorting procedure for the same data from which Fig. 1*A* was selected is shown in three stages in Fig. 1*C*. Each histogram represents the distribution of the population of action potentials as a function of dissimilarity number; the waveform used as "standard" is shown for each stage in the calculation. In the first stage of separation, the population is divided at the arrow into two groups: left peak, those waveforms most similar to the "standard" shown; and right peak, all other waveforms. All waveforms that fall into the left peak are labeled type 0 and removed from the data. In the second stage of separation, the remaining population is again divided into two groups; the waveforms that fall into the left peak are labeled type 1 and

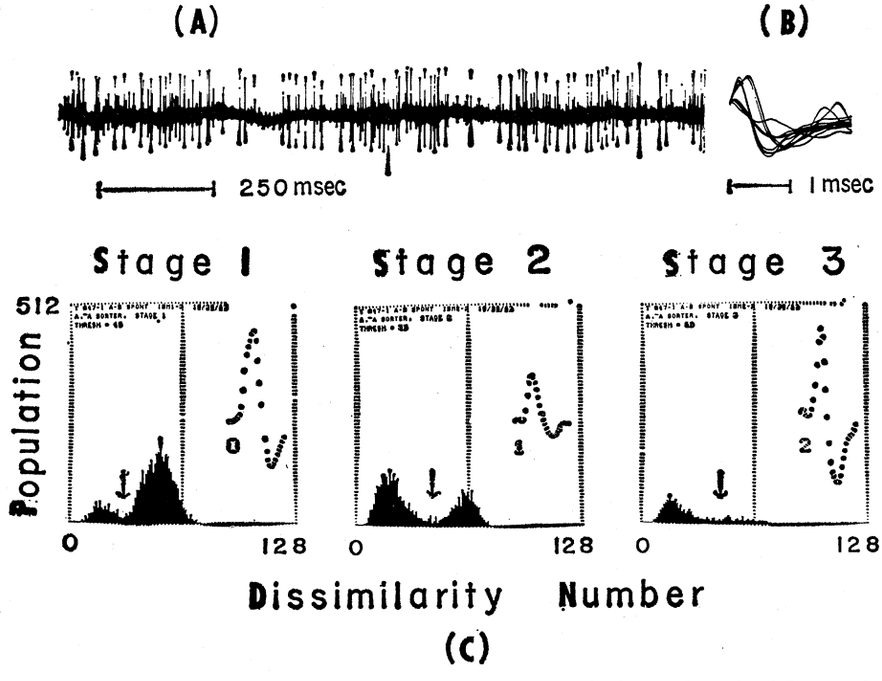

Fig. 1. Action potentials from several adjacent neurons. *A*, Approximately 1.5 seconds of action potential data from several units. *B*, Multiple triggered sweeps of an oscilloscope at high speed to show the three waveforms of action potentials in the data. *C*, Population as a function of dissimilarity number during three stages of the separation (see text).

removed from the data. The remaining population of waveforms falls mainly into one peak, as shown in the third stage. Those waveforms that fall to the left of the arrow are labeled type 2. The residue to the right of the arrow represents various anomalous waveforms arising when two different action potentials almost coincide in time.

A print-out for monitoring the final sorting of the data is shown in Fig. 2; each action potential was labeled by the computer. Errors in classification generally run well under 5 percent and the entire procedure takes several minutes.

Once the action potentials have been sorted, it is easy to examine the statistical properties of the firing patterns of each neuron in the recording as well as the various conditional firing probabilities which can be used for examining interactions between different neurons. A current study of the dorsal cochlear nucleus by these means shows that contiguous neurons interact in various ways that depend partly on the parameters of the stimulus.

G. L. GERSTEIN
W. A. CLARK
Center for Computer Technology and Research in the Biomedical Sciences, Massachusetts Institute of Technology, Cambridge

References and Notes

1. T. P. S. Powell and V. B. Mountcastle, *Bull. Johns Hopkins Hosp.* **105**, 108 (1959); J. E. Hind, J. E. Rose, P. W. Davies, C. N. Woolsey, R. M. Benjamin, W. S. Welkes, R. F. Thompson, in *Neural Mechanisms of the Auditory and Vestibular Systems*, G. L. Rasmussen and W. F. Windle, Eds. (Thomas, Springfield, Ill., 1960).
2. D. H. Hubel and T. N. Wiesel, *J. Physiol.* **160**, 106 (1962).
3. V. B. Mountcastle, *J. Neurophysiol.* **20**, 408 (1957); ——— and T. P. S. Powell, *Bull. Johns Hopkins Hosp.* **105**, 173 (1959).
4. V. E. Amassian, L. Berlin, J. Macy, H. J. Waller, *Trans. N.Y. Acad. Sci., Ser. II* **21**, 395 (1959); M. Verzeano and K. Negishi, *J. Gen. Physiol.* **43** (*Suppl.*), 177 (1960).
5. D. H. Hubel, *Science* **125**, 549 (1957).
6. Lepel High Frequency Laboratories, Woodside, L.I., N.Y., Type E2. For this type of coil, an input of 20 volts with a duration of 100 ms gives adequate results.
7. J. S. Griffith and G. Horn, *Nature* **199**, 876 (1963).
8. Recent work at this laboratory by W. Simon has shown that similar data processing can also be done, although at some cost in time, with the LINC, a small computer intended for use in the laboratory.
9. We thank the staffs of the Research Laboratory of Electronics, M.I.T., and of the TX-2 computer at Lincoln Laboratory, M.I.T., for their technical assistance. This research was supported in part by U.S. Army Signal Corps, the Air Force Office of Scientific Research, and the Office of Naval Research; the National Institutes of Health (grants FR-00142-01 and MH 04737-03); and the National Science Foundation (grant G-16526).

3 January 1964

Conglutination: Specific Inhibition by Carbohydrates

Abstract. *Conglutination of antigen-antibody-complement complexes is inhibited by a number of acetamido sugars, the most efficient being* N-*acetyl*-D-*glucosamine and closely related compounds. The effects of structural modification on activity of* N-*acetyl*-D-*glucosamine are described.*

Chromatographically purified bovine conglutinin (*1*) clumps, or conglutinates, complexes of antigen, antibody, and complement. It has been suggested that this conglutination reaction is due to combination of conglutinin with sites on a component or components of complement which are only exposed after binding to the antigen-antibody aggregate (*2*). To elucidate the chemical basis of specificity of the conglutinin system we have examined a variety of carbohydrates for possible inhibitory activity.

The results (Table 1) suggest that a molecule containing an acetamido sugar plays an important role in determining specificity of the conglutination reaction. A feature of all inhibitory acetamido sugars is the sequence

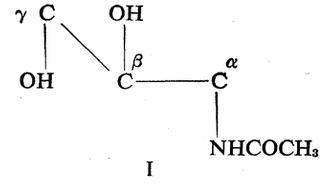

I

In the case of 3-acetamido-3-deoxy-D-galactose, 3-acetamido-3-deoxy-D-manno-D-galaheptose, and 3-acetamido-3-deoxy-D-glucose, all weak inhibitors, the γ carbon is the anomeric carbon. α-Glycosides of these sugars should therefore be inactive if the structural sequence I is an absolute requirement for inhibition by acetamido sugars.

A progressive decrease in activity of *N*-acetyl-D-glucosaminides, which paralleled the change in size of substituents, was observed in the series

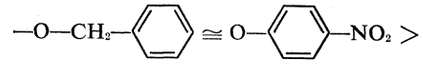

$$-O-C_2H_5 > -O-CH_3.$$

Subsitution of an *N*-butyryl group for *N*-acetyl of *N*-acetyl-D-glucosamine had little effect on activity whereas substitution of *N*-carboxymethyl or amino for *N*-acetyl markedly reduced or completely abolished activity. Replacement of $-CH_2OH$ at carbon atom 6 of *N*-acetyl-D-glucosamine by either —H or $-CH_2$-*O*-β-D-galactose also diminished the inhibitory activity. The 4-*O*-β-D-galactoside was inactive.

The assessment of significance to the weak reactivity displayed by L-fucose and 3-*O*-methyl-L-fucose is difficult at present. However, it is noteworthy that 2-*O*-methyl-L-fucose as well as all the D-fucose derivatives tested were inactive.

Certain sugars could not be tested for inhibitory activity because they ag-

Table 1. Inhibition of conglutination by carbohydrate. The test system contained 0.1 ml of conglutinin dilution, 0.1 ml of sheep erythrocyte-antibody-complement complex (*1*), and 0.3 ml of sugar in buffered saline. The mixture was incubated at 32°C for 30 minutes.

Sugar	Molarity required for inhibition
N-Acetyl-D-glucosamine	0.0004–0.0008
Chitobiose*	
N-Butyryl-D-glucosamine†	
6-*O*-β-D-Galactosyl-*N*-acetyl-D-glucosamine‡	0.0014–0.003
p-Nitrophenyl-2-acetamido-2-deoxy β-D-glucoside*	
Benzyl-2-acetamido-2-deoxy-α-D-glucoside§	
Benzyl-2-acetamido-2-deoxy-β-D-glucoside§	
Ethyl-2-acetamido-2,6-dideoxy-β-D-glusoside‡	0.060
Ethyl-2-acetamido-2-deoxy-β-D-glucoside‡	
3-Acetamido-3-deoxy-D-manno-D-galaheptose‡	
3-Acetamido-3-deoxy-D-glucose‡	
3-Acetamido-3-deoxy-D-galactose‡	
2-Acetamido-2-deoxy-D-xylose‡	
N-Carboxymethyl-D-glucosamine‡	
L-Fucose‖	
3-*O*-Methyl-L-fucose‖	
D-Glucosamine	Inactive
D-Glucosaminic acid¶	
Muramic acid#	
4-Acetamido-4-deoxy-D-glycero-L-galaoctose‡	
4-Acetamido-4-deoxy-D-glycero-L-idooctose‡	
3-Acetamido-3-deoxy-D-gluco-D-idoheptose‡	
3-Acetamido-3-deoxy-D-gluco-D-guloheptose‡	
Methyl-2-acetamido-2-deoxy-α-D-glucoside**	
Methyl-2-acetamido-2-deoxy-β-D-glucoside‡,**	
Methyl-3-acetamido-3-deoxy-D-manno-D-galaheptose‡	
2-Acetamido-2-deoxy-D-galactose‡	
2-Acetamido-2-deoxy-D-gulose‡	
2-Acetamido-2-deoxy-D-arabinose‡	
2-Acetamido-2-deoxy-D-ribose‡	
2-Acetamido-2-deoxy-D-mannose††	
2-*N*-Isopropyl-2-deoxy-L-glucosamine‡	
2-Acetamido-2-deoxy-D-sorbitol‡	
1-Acetamido-1-deoxy-D-glucitol¶	
2-*O*-Methyl-L-fucose‖	
D-Fucose‖	
Methyl-α-D-fucoside‖	
2-*O*-Methyl-D-fucose‖	
3-*O*-Methyl-D-fucose‖	
All common nonnitrogen containing mono- and disaccharides except L-fucose and 3-*O*-methyl-L-fucose	

Kindly supplied by: * O. Lüderitz, † K. Onodera, ‡ R. Kuhn, § H. K. Zimmerman, ‖ G. Springer, ¶ M. Wolfrom, # R. Gigg, ** F. Zilliken, †† S. Roseman.